

Functional analysis of Fontan energy dissipation

Lakshmi P. Dasi^a, Kerem Pekkan^b, Hiroumi D. Katajima^a, Ajit P. Yoganathan^{a,*}

^aWallace H. Coulter School of Biomedical Engineering, Georgia Institute of Technology, Atlanta, GA 30332-0535, USA

^bDepartment of Biomedical and Mechanical Engineering, Carnegie Mellon University, Pittsburgh, PA, USA

Accepted 14 April 2008

Abstract

We formalize the hydrodynamic energy dissipation in the total cavopulmonary connection (TCPC) using dimensional analysis and examine the effect of governing flow variables; namely, cardiac output, flow split, body surface area, Reynolds number, and certain geometric characteristics. A simplistic and clinically useful mathematical model of the dependence of energy dissipation on the governing variables is developed. *In vitro* energy loss data corresponding to six patients' anatomies validated the predicted dependency of each variable and was used to develop a predictive, semi-empirical energy dissipation model of the TCPC. It is shown that energy dissipation is a cubic function of pulmonary flow split in the physiological range. Furthermore, non-dimensional energy dissipation, which is a measure of resistance of the connection, is dependent on Reynolds number and geometrical factors alone. Non-dimensional energy dissipation decreases with Reynolds number as $Re^{-0.25}$ ($R^2 > 0.95$). In addition, for high Reynolds numbers, within physiological exercise limits, dissipation strongly correlates to minimum PA area as a power law decay with an exponent of $-5/4$ ($R^2 > 0.88$). This study presents a simple analytical form of energy dissipation rate in complex patient-specific TCPCs that accurately captures the effect of cardiac output, flow split, body surface area, Reynolds number, and pulmonary artery size within physiological limits. Further studies with larger sample sizes are necessary for incorporating finer geometrical parameters such as vessel curvatures and offsets.

© 2008 Elsevier Ltd. All rights reserved.

Keywords: Fontan; Powerloss; Energy dissipation; Head loss; Total cavopulmonary connection; Vessel junction

1. Introduction

The Fontan procedure is a palliative cure for children born with a single functional ventricle (Fontan and Baudet, 1971). This surgical procedure involves the routing of venous blood from superior vena cava (SVC) and inferior vena cava (IVC) directly to the left and right lungs through an *in situ* surgically fabricated vascular connection. The present and most popular form of this complex connection is the total cavopulmonary connection (TCPC) (Deleval et al., 1988), which has a “+”-shaped vascular topology. Since the entire circulation system of these patients is driven by the single ventricle pump, energy optimization is crucial for long lasting benefits to the patient (Senzaki et al., 2002, Sundareswaran et al., 2007).

To illustrate the importance of energy savings in the single ventricle physiology, previous studies have shown that certain geometric characteristics of the TCPC and the

associated vessels, mainly the pulmonary arteries (PA), play an important role in determining the short-term and long-term patient outcomes (Hosein et al., 2007; Pekkan et al., 2004; Sung et al., 1998; Walker et al., 2000, 2001). Factors such as PA stenosis degrade the flow efficiency and increase the risk factor for Fontan failure (Sung et al., 1998). *In vitro* studies have highlighted the importance of curvature of the IVC, and its offset relative to the SVC in minimizing the energy dissipation at idealized TCPC junctions (Ensley et al., 1999; Ryu et al., 2001). Furthermore, most recent efforts aim to differentiate between the energetic efficiency of different types of TCPCs (Whitehead et al., 2007).

Despite these and numerous other studies (Grigioni et al., 2006; Venkatachari et al., 2007), there exists no formal analysis of the TCPC energy dissipation problem from a fundamental fluid mechanics stand point. In all previous studies, energy dissipation has always been a measured *in vivo*, *in vitro*, or computed quantity and, to the best of our knowledge, none of them have attempted to describe the functional dependence with respect to cardiac output, body surface area, Reynolds

*Corresponding author. Tel.: +1 404 894 2849; fax: +1 404 894 4243.

E-mail address: ajit.yoganathan@bme.gatech.edu (A.P. Yoganathan).

number, or geometric factors. A fundamental understanding of how energy dissipation is related to these governing factors is crucial in order to develop a proper framework that will enable unbiased comparisons between TCPCs of different patients through proper indexing of measurements. In this study, we formalize the energy dissipation problem in the TCPC using dimensional analysis and examine the effect of governing variables namely cardiac output, flow split, body surface area, Reynolds number, and certain geometric characteristics. Doing so, we present a simple analytical form of energy dissipation rate in complex patient-specific TCPCs that accurately captures the effect of all governing variables within physiological limits of these variables.

2. Materials and methods

Anatomically accurate *in vitro* models of six patient TCPCs were fabricated and the energy dissipation rate was experimentally determined for the steady flow conditions shown in Table 1. All patients were imaged either at the Children's Hospital of Atlanta (CHOA), or Children's Hospital of Philadelphia (CHOP). Fig. 1 depicts the reconstructed TCPC geometries of these six patients labeled by their respective patient IDs in the Fontan database at Georgia Tech. Informed consent was obtained from all patients and all study protocols complied with the Institutional Review Boards of the participating hospitals and the Georgia Institute of Technology. The lowest cardiac outputs (Table 1) correspond to resting conditions evaluated from the respective PC MRI data, while higher cardiac outputs simulated exercise conditions.

Details of the experimental methodology to determine the hydrodynamic energy dissipation characteristics of anatomic TCPCs can be found in literature (de Zelicourt et al., 2005a, b; Kitajima, 2007). Briefly TCPC blood volumes were reconstructed from anatomic MRI data and physical models manufactured using rapid-prototyping technology with a transparent resin. The physical models of the patient-specific TCPCs with two inlets (IVC and SVC) and two outlets (PAs) were connected to a steady flow loop for pressure drop measurements. The flow was driven by gravity head provided by a constant head tank. The tank maintained head using a steady flow pump which continuously refilled the tank. The working fluid used was a mixture of water and glycerin to provide a Newtonian approximation of blood with a kinematic viscosity of $3.5 \times 10^{-6} \text{ m}^2/\text{s}$. The flow conditions shown in Table 1 were achieved with the help of three gate valves (one to control the total cardiac output, another to split the total flow 60:40 ratio for IVC:SVC inflow, and the third valve to impose the desired pulmonary flow split). All flow rates were measured using calibrated rotameters, while pressures at each of the vessels in the vicinity of the TCPC were measured using static differential pressure transducers.

3. Results

In this section, we first outline the fluid mechanical formulation of energy dissipation in a two-inlet, two-outlet

Table 1
Flow conditions used in the evaluation of power loss

Patient	Flow conditions (L/min)
CHOA007	2, 3 and 4
CHOA008	2, 3 and 4
CHOP013	2, 3 and 4
CHOA009	2, 3 and 4
CHOA011	4, 5, 6 and 7
CHOP034	4, 5.2, 6.4 and 7.6

TCPC connection using dimensional analysis. The formulation leads to a simplistic analytical form of energy dissipation, with the incorporation of a few assumptions. The analytical form is compared against *in vitro* data to yield a semi-empirical model that captures the basic dependencies of each governing variable. The significance of these results is later discussed in the discussion section.

3.1. Dimensional analysis

Let ε (watts) be the time-averaged energy dissipation rate due to the viscous and form friction that blood flow encounters in the TCPC. The functional dependence of ε in all its generality can be expressed as

$$\varepsilon = F(Q, \alpha, \rho, \mu, \text{BSA}, S_i) \quad (1)$$

where Q is the cardiac output, α is the % flow split defined as the fraction of the cardiac output flowing to the left lung, ρ is the density of blood, μ is the blood viscosity, BSA is the patient body surface area, and S_i is a vector quantity that is a parametric representation of the TCPC geometry.

According to the Buckingham π theorem (Buckingham, 1914), Eq. (1) can be reduced to an equivalent relationship between dimensionless groups. Applying the theorem, it can be shown that Eq. (1) in its dimensionless form reduces to

$$\frac{\varepsilon}{\rho(Q^3/\text{BSA}^2)} = f(\alpha, Re, S'_i) \quad (2)$$

where Re is the Reynolds number and S'_i is a dimensionless parametric representation of the TCPC geometry.

3.2. Simplification and assumptions

The following steps outline how the above-dimensional analysis result (Eq. (2)) can be used to develop an analytical model of energy dissipation:

- (1) Total power loss can be expressed as the sum of power lost by the flow headed to the left lung, ε_L , and that lost by flow headed to the right lung, ε_R , as follows:

$$\varepsilon = \varepsilon_L + \varepsilon_R \quad (3)$$

- (2) Applying dimensional analysis on the flow within the TCPC headed to the left lung gives

$$\frac{\varepsilon_L}{\rho(\alpha^3 Q^3/\text{BSA}^2)} = f(Re, S'_{iL}) \quad (4)$$

- (3) Applying dimensional analysis similarly to the flow towards the right lung gives

$$\frac{\varepsilon_R}{\rho((1-\alpha)^3 Q^3/\text{BSA}^2)} = f(Re, S'_{iR}) \quad (5)$$

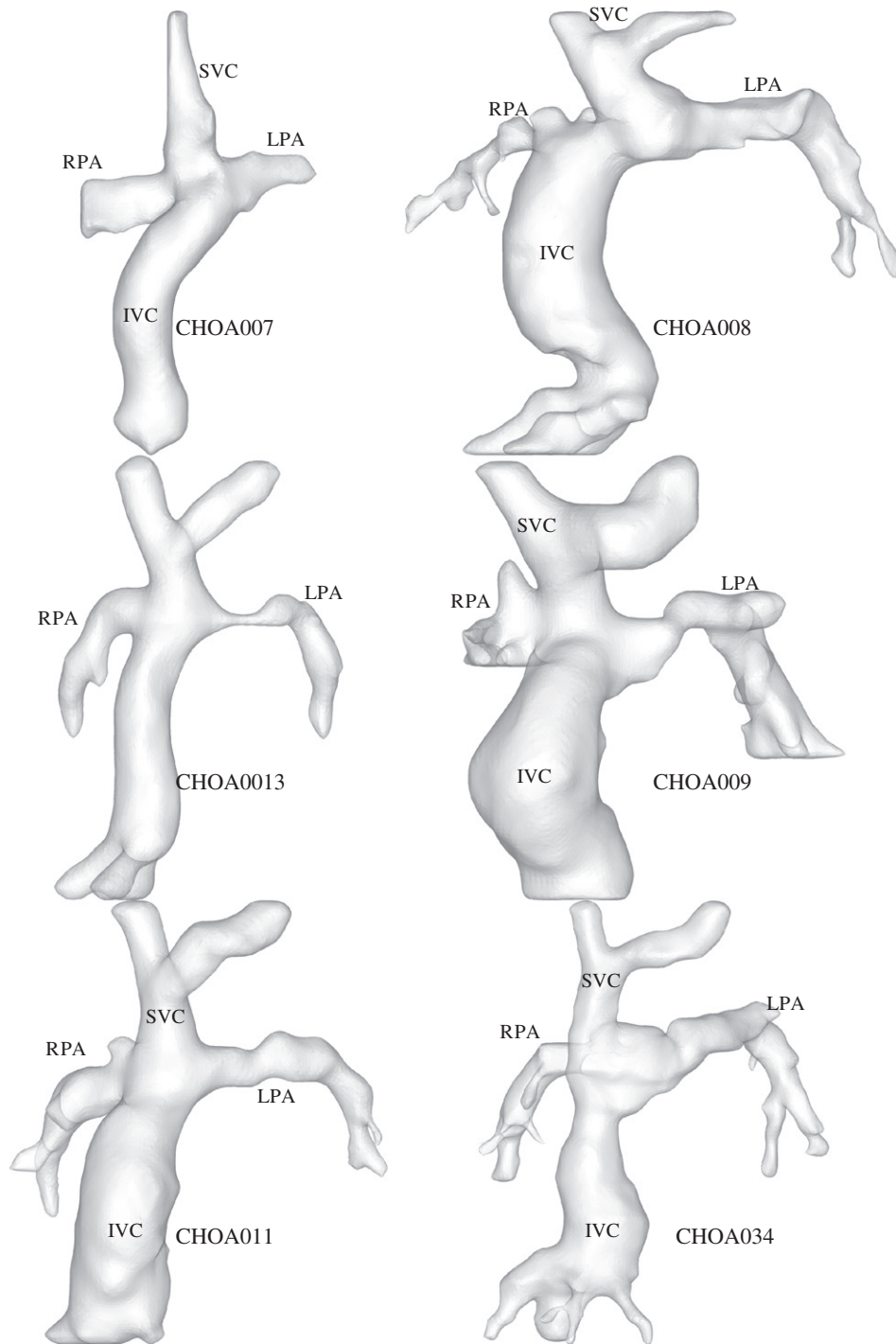


Fig. 1. Anatomic reconstructions of six patients used in *in vitro* energy dissipation measurements.

(4) Substituting Eqs. (4) and (5) into (3) gives

$$\frac{\epsilon}{\rho(Q^3/BSA^2)} = \alpha^3 f(Re, S'_{iL}) + (1 - \alpha)^3 f(Re, S'_{iR}) \quad (6)$$

(5) Assume that the function $f(\cdot)$ can be decomposed by separation of variables such that

$$f(Re, S'_i) = \psi(Re)\zeta(S'_i) \quad (7)$$

(6) Substituting (7) into (6) gives

$$\frac{\epsilon}{\rho(Q^3/BSA^2)} = \psi(Re)[\alpha^3 \zeta(S'_{iL}) + (1 - \alpha)^3 \zeta(S'_{iR})] \quad (8)$$

Eq. (8) is the analytical representation of energy dissipation in the TCPC with unknown functions $\psi(Re)$ and $\zeta(S'_i)$ that are empirically determined (next section) from the *in vitro* data.

3.3. Empirical data

The analytical expression for energy dissipation within the TCPC shows that the dimensionless energy dissipation is dependent on flow split, Reynolds number and geometric shape factors. In particular, assumption (1) directly implies that the dependence of energy dissipation with respect to flow split is a cubic function. Specifically, if one were to define imaginary (i.e., non-physiological) energy dissipation states at $\alpha = 0$ and 100 as P_L and P_R , respectively, then energy dissipation at any arbitrary α is given by the interpolation

$$\varepsilon = P_L\alpha^3 + P_R(1 - \alpha)^3 \tag{9}$$

Fig. 2 shows the measured energy dissipation plotted as a function of flow split for each cardiac output as noted in Table 1. For each flow condition, a least square best fit using Eq. (9) is performed and has also been plotted along with the raw data (Fig. 2). The R^2 values for all the best fit plots were greater than 0.98.

In order to examine Reynolds number dependence (i.e., $\psi(Re)$ only) P_L and P_R , calculated as intercepts of the best fit curve (Eq. (9)) at $\alpha = 0,100$, respectively, were plotted as a function of Reynolds number (based on total cardiac

output and IVC size). Each P_L and P_R vs. Re curve, corresponding to a patient and flow split condition, was multiplied by a constant, such that all the curves plotted collapsed to an imaginary power law function with minimum square error. This process allows for the quantification of power law behavior, if any. Fig. 3 shows this data with the arbitrary-scaled P_L and P_R vs. Reynolds number on a log–log plot. A clear power law behavior with an exponent of 2.75 emerged for Reynolds number greater than about 1000. Since, from Eq. (2), energy dissipation already scales with flow rate as $\propto Q^3$, this implies that $\psi(Re)$ is actually $\propto Re^{-0.25}$. The significance of this result is discussed in the next section.

Modeling the function $\xi(S'_i)$, first requires the definition of the parametric variable S . Our previous work has identified several geometric characteristics that can be used to describe any patient-specific TCPC (KrishnankuttyRema et al., 2008). It was shown that minimum PA cross-sectional sizes strongly differentiated between different types of TCPCs; therefore, with a sample size of six, we examine only the PA size factor using the minimum PA areas calculated in our previous work (KrishnankuttyRema et al., 2008). Fig. 4 shows the variation of P_L and P_R for exercise conditions normalized by the factor $\rho Q^3/BSA^2Re^{-0.25}$ with

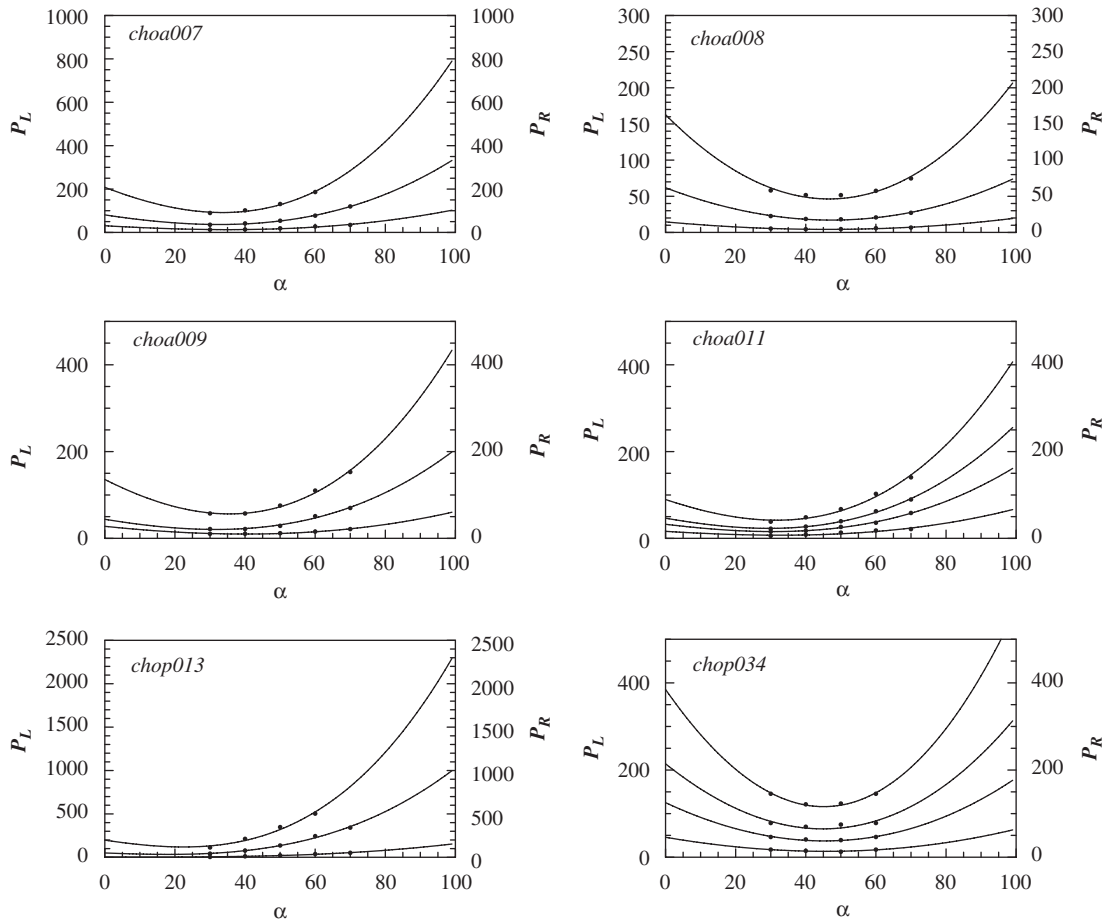


Fig. 2. *In vitro* energy dissipation measurements for the six patient-specific TCPCs at varying flow rates ranging from resting cardiac output to exercise condition. Also plotted is the least square fit of Eq. (9). R^2 values of all least square fits were >0.98 .

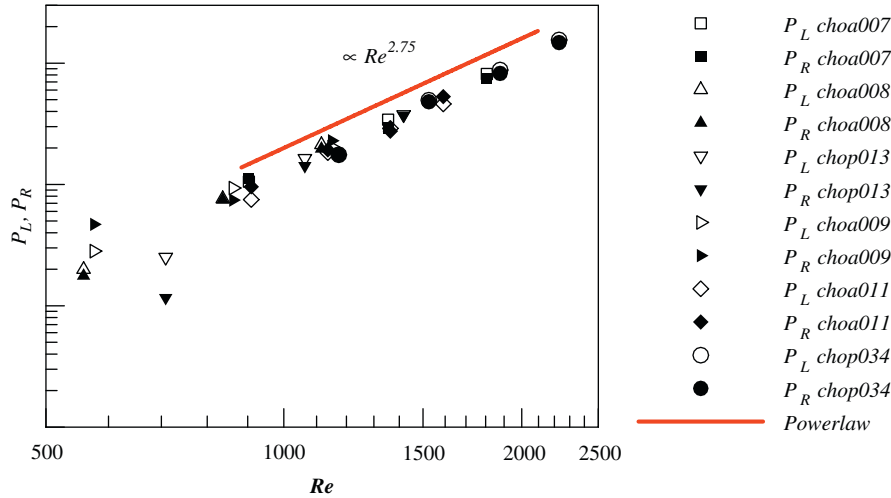


Fig. 3. Arbitrarily-scaled energy dissipation intercepts, P_L and P_R , plotted as a function of Reynolds number. Note the power law behavior under exercise conditions.

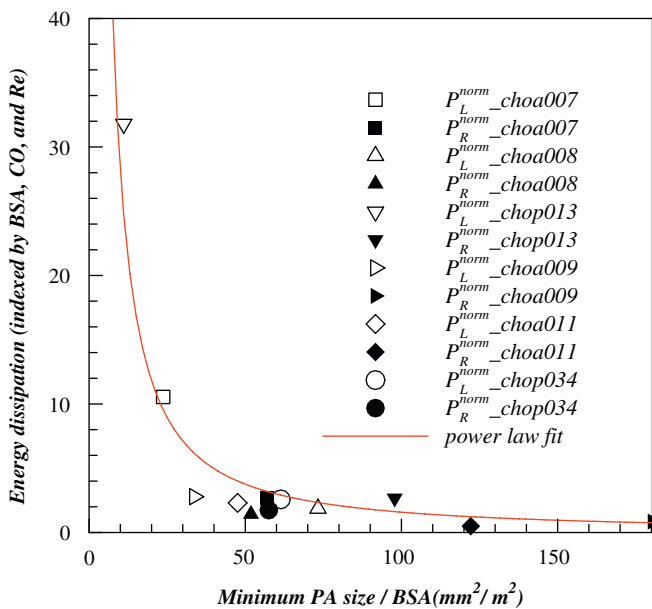


Fig. 4. P_L and P_R normalized to dynamic power and indexed for Reynolds number variation under maximum exercise condition plotted as a function of minimum PA size. Note the power law dependence.

respect to normalized PA sizes, i.e., normalized minimum left PA area or right PA area, respectively. This data showed the strongest correlation between P_L and P_R and the bottleneck regions defined on the PAs. The data closely followed a power law ($R^2 > 0.92$, $p < 0.05$) with an exponent of -1.25 .

4. Discussion

This study is the first comprehensive attempt to understand the functional relationships between hemodynamic energy dissipation that occurs within the TCPC and governing variables; namely, cardiac output, flow split, BSA, and certain geometric factors, such as minimum PA

size. Dimensional analysis yielded that energy dissipation is directly proportional to the dynamic (kinetic) power scale given by $\rho(Q^3/BSA^2)$. This factor is similar to the total kinetic power derived previously (Milnor et al., 1966). However, Eq. (2) shows that the proportionality to the power scale is dependent on the flow split, Reynolds number, as well as geometry as expected.

4.1. Flow split dependence

Assumption (1), which decomposed the TCPC into two separate two-inlet, one-outlet (i.e., mixing Tee junctions) connections, yielded that the variation with flow split must be of the form given in Eq. (9). In reality, this assumption is counterintuitive as there exists a strongly non-linear coupling between the flow heading to the left lung and the right lung inside the TCPC. Studies have shown that the flow collision between the vena caval streams causes an unsteady mixing zone at the center of the “+”-shaped connection. Nevertheless, the excellent fit of the cubic variation on the measured energy dissipation from the *in vitro* data over physiological ranges of flow split (i.e., 30–70%) shows that the non-linear interaction may be weak in the sense that the power losses may be dominated by the losses occurring due to the sudden changes in vessel sizes (vena cava to PAs). The behavior captured the flow split dependence well for various cardiac outputs, as well as those with severe stenosis. For instance, see Fig. 2 for the case of CHOP013, which is a case of severe left PA stenosis (Fig. 1).

Note that assumption (1) may very well break down as flow split approaches 0% or 100% and the function may depart from the cubic behavior. This study is unable to examine the validity of the cubic behavior over the full range because excessive energy dissipation occurs at extreme flow splits, which our constant tank facility was unable to overcome. Nevertheless, Eq. (9) shows the

potential significance of non-physiological conditions that may govern the physics over physiological ranges.

4.2. Reynolds number dependence

From Fig. 3, it is clear that as Reynolds number increases with patient exercise, the non-linear increase in energy dissipation approaches a power law behavior with an exponent of 2.75. However, note that in this figure, energy dissipation has not been normalized with the dynamic power scale, which scales with cardiac output as $\propto Q^3$. This implies that the pure Reynolds number dependence of the non-dimensional energy dissipation, $\psi(Re)$, scales as $\propto Re^{-0.25}$, i.e., the non-dimensional energy dissipation actually decreases weakly with Reynolds number. This compares well with the behavior of internal friction factor (Blasius, 1911), which is also known to reduce with Reynolds number under turbulent conditions as $\propto Re^{-0.25}$ for moderate Reynolds numbers but not fully developed turbulent conditions. The behavior also corroborates well with the decreasing non-dimensional energy dissipation studied in a recent computational investigation of TCPC resistance of extra-cardiacs and intra-atrial TCPCs (Whitehead, et al., 2007).

4.3. Geometry dependence

From this study, only the effect of minimum PA sizes on the energy dissipation function could be established. Fig. 4 shows that as the minimum cross-sectional areas of the PA decrease, energy dissipation increases non-linearly in a power law manner. The power law exponent was empirically determined to be -1.25 . In order to determine the dependence with other parameters such as vessel orientations, angles, curvatures, etc., further studies need to be conducted with large sample sizes.

5. Significance

Despite the small sample size, the study establishes an important analytical form of energy dissipation in the TCPC that has profound significance in all clinical studies involving the comparison of TCPC energy dissipation. The analytical form allows the proper definition of TCPC resistance and thus a means for unbiased comparisons. It has been shown that the TCPC energy dissipation for physiological hemodynamic conditions can be expressed as

$$\varepsilon = \rho \frac{Q^3}{BSA^2} \left[C_{\text{left}} \left(\frac{A_{\text{lpa}}}{BSA} \right)^{-1.25} \alpha^3 + C_{\text{right}} \left(\frac{A_{\text{rpa}}}{BSA} \right)^{-1.25} (1 - \alpha)^3 \right] Re^{-0.25} \quad (10)$$

where C_{left} and C_{right} are flow, Reynolds number, and PA size-independent resistance coefficients that are pure functions of other geometric factors such as curvatures, angles, and orientations of the vessels; and A_{lpa} and A_{rpa} are minimum PA cross-sectional areas. Based on Eq. (10), the energy dissipation of the entire pulmonary circuit is

given by the equation

$$E_{\text{pulmonary}} = \rho \frac{Q^3}{BSA^2} \times \left[C_{\text{left}} \left(\frac{A_{\text{lpa}}}{BSA} \right)^{-1.25} \alpha^3 + C_{\text{right}} \left(\frac{A_{\text{rpa}}}{BSA} \right)^{-1.25} (1 - \alpha)^3 \right] Re^{-0.25} + Q^2 [\alpha^2 L_L + (1 - \alpha)^2 L_R] \quad (11)$$

where $E_{\text{pulmonary}}$ is the energy dissipation of the entire pulmonary circuit and L_L and L_R are the resistances of the left and right lungs, respectively. Eq. (11) also defines the operating flow split, α_o , governed by the path of least resistance as

$$\left. \frac{dE_{\text{pulmonary}}}{d\alpha} \right|_{\alpha=\alpha_o} = 0 \quad (12)$$

6. Conclusions

Dimensional analysis of energy dissipation in the TCPC has been performed and a simplistic, semi-empirical model developed that captures the dependence of governing variables such as cardiac output, flow split, Reynolds number, and minimum PA size under exercise conditions.

Conflict of interest statement

There is no conflict of interest.

Acknowledgment

The authors gratefully acknowledge the funding from National Heart, Lung and Blood Institute (HL67622).

References

- Blasius, H., 1911. The similarity law in friction processes. *Physikalische Zeitschrift* 12, 1175–1177.
- Buckingham, E., 1914. On physically similar systems, illustrations of the use of dimensional equations. *Physical Review* 4 (4), 345–376.
- de Zelicourt, D., Pekkan, K., Kitajima, H., Frakes, D., Yoganathan, A.P., 2005a. Single-step stereolithography of complex anatomical models for optical flow measurements. *Journal of Biomechanical Engineering—Transactions of the ASME* 127 (1), 204–207.
- de Zelicourt, D.A., Pekkan, K., Wills, L., Kanter, K., Forbess, J., Sharma, S., Fogel, M., Yoganathan, A.P., 2005b. In vitro flow analysis of a patient-specific intra-atrial total cavopulmonary connection. *Annals of Thoracic Surgery* 79 (6), 2094–2102.
- Devalal, M.R., Kilner, P., Gewillig, M., Bull, C., 1988. Total cavopulmonary connection—a logical alternative to atriopulmonary connection for complex Fontan operations—experimental studies and early clinical-experience. *Journal of Thoracic and Cardiovascular Surgery* 96 (5), 682–695.
- Ensley, A.E., Lynch, P., Chatzimavroudis, G.P., Lucas, C., Sharma, S., Yoganathan, A.P., 1999. Toward designing the optimal total cavopulmonary connection: an in vitro study. *Annals of Thoracic Surgery* 68 (4), 1384–1390.
- Fontan, F., Baudet, E., 1971. Surgical repair of tricuspid atresia. *Thorax* 26 (3), 240.
- Grigioni, M., D’Avenio, G., Amodeo, A., Di Donato, R.M., 2006. Power dissipation associated with surgical operations’ hemodynamics: critical

- issues and application to the total cavopulmonary connection. *Journal of Biomechanics* 39 (9), 1583–1594.
- Hosein, R.B.M., Clarke, A.J.B., McGuirok, S.P., Griselli, M., Stumper, O., De Giovanni, J.V., Barron, D.J., Brawn, W.J., 2007. Factors influencing early and late outcome following the Fontan procedure in the current era. The ‘Two Commandments’? *12*, 344–353.
- Kitajima, H.D., 2007. In vitro Fluid Dynamics of Stereolithographic Single Ventricle Congenital Heart Defects from In Vivo Magnetic Resonance Imaging. Georgia Institute of Technology, Atlanta, GA.
- KrishnankuttyRema, R., Dasi, L.P., Pekkan, K., Sundareswaran, K., Fogel, M., Sharma, S., Kanter, K., Spray, T., Yoganathan, A.P., 2008. Quantitative analysis of extracardiac versus intra-atrial Fontan anatomic geometries. *Annals of Thoracic Surgery* 85 (3), 810–817.
- Milnor, W.R., Bergel, D.H., Bargaine, Jd., 1966. Hydraulic power associated with pulmonary blood flow and its relation to heart rate. *Circulation Research* 19 (3), 467.
- Pekkan, K., de Zelicourt, D., Kitajima, H., Forbess, J.M., Kanter, K.R., Parks, J.W., Sharma, S., Fogel, M.A., Yoganathan, A.P., 2004. Functional left pulmonary artery stenosis in total cavopulmonary connection (TCPC): assessing improvements in lung perfusion and cardiac workload with computer-aided angioplasty. *Circulation* 110 (17), 737.
- Ryu, K., Healy, T.M., Ensley, A.E., Sharma, S., Lucas, C., Yoganathan, A.P., 2001. Importance of accurate geometry in the study of the total cavopulmonary connection: computational simulations and in vitro experiments. *Annals of Biomedical Engineering* 29 (10), 844–853.
- Senzaki, H., Masutani, S., Kobayashi, J., Kobayashi, T., Sasaki, N., Asano, H., Kyo, S., Yokote, Y., Ishizawa, A., 2002. Ventricular afterload and ventricular work in Fontan circulation-comparison with normal two-ventricle circulation and single-ventricle circulation with blalock-taussig shunts. *Circulation* 105 (24), 2885–2892.
- Sundareswaran, K. S., Pekkan, K., Dasi, L. P., Kitajima, H. D., Whitehead, K., Fogel, M. A., and Yoganathan, A. P., 2007. Significant impact of the total cavopulmonary connection resistance on cardiac output and exercise performance in single ventricles. *Circulation* 116(16_MeetingAbstracts), p. 479.
- Sung, H.W., Hsu, T.L., Hsu, C.H., Hsu, J.C., 1998. Pulmonary artery hemodynamics with varying degrees of valvular stenosis: an in vitro study. *Journal of Biomechanics* 31 (12), 1153–1161.
- Venkatachari, A.K., Halliburton, S.S., Setser, R.M., White, R.D., Chatzimavroudis, G.P., 2007. Noninvasive quantification of fluid mechanical energy losses in the total cavopulmonary connection with magnetic resonance phase velocity mapping. *Magnetic Resonance Imaging* 25 (1), 101–109.
- Walker, P.G., Howe, T.T., Davies, R.L., Fisher, J., Watterson, K.G., 2000. Distribution of hepatic venous blood in the total cavopulmonary connection: an in vitro study. *European Journal of Cardio-Thoracic Surgery* 17 (6), 658–665.
- Walker, P.G., Oweis, G.F., Watterson, K.G., 2001. Distribution of hepatic venous blood in the total cavopulmonary connection: an in vitro study into the effects of connection geometry. *Journal of Biomechanical Engineering—Transactions of the ASME* 123 (6), 558–564.
- Whitehead, K.K., Pekkan, K., Doddasomayajula, R., Kitajima, H.D., Sundareswaran, K.S., Paridon, S.M., Yoganathan, A.P., Fogel, M.A., 2007. Computational model of exercise effects on Fontan hemodynamics demonstrates favorable energetics in extracardiac fontans when compared to lateral tunnel. *Circulation* 116 (16), 481.